Tran et al. Animal Biotelemetry (2024) 12:12
https://doi.org/10.1186/s40317-024-00369-y

Animal Biotelemetry

METHODOLOGY

Open Access

Evaluating habitat-specific interference in automated radio telemetry systems: implications for animal movement studies

Vinh T. Tran[1], Andrew C. Vitz[2] and Marja H. Bakermans[1,3*]

Abstract

Automated radio telemetry systems have become a popular and invaluable tool in tracking the activity and movement of wild animals. However, many environmental conditions can hinder accuracy when tracking with this technology. For instance, study sites may contain multiple habitat types, each habitat uniquely affecting the signal strength received from tagged species. To investigate the influence of a structurally diverse study site on an automated radio telemetry system, we conducted this project at a restored and managed pine barren habitat that consisted of a mix of mature pitch pine, treated pitch pine, scrub oak, and hardwood forests. This site, Montague Plains Wildlife Management Area, Montague, Massachusetts, is also a known breeding ground for Eastern whip-poor-will (*Antrostomus vociferus*). To measure the relationship of radio signal strength with distance across each habitat, we used radio telemetry equipment manufactured by Cellular Tracking Technologies. We produced negative exponential decay functions measuring radio signal strength over distance and tested for differences among habitat types on radio signal strength (RSS). We found that decay function parameters significantly differed by habitat type, prompting us to investigate if accounting for these differences improved location estimate accuracy. To test this, we estimated known locations using trilateration methods with and without habitat calibration. Comparing these tests indicates that habitat-specific adjustments significantly improved location accuracy. Lastly, we visualized estimated RSS-based locations of 1 week of whip-poor-will data and compared them to GPS data generated from the same individual. Previous studies have accounted for types of environmental interference (like elevation) in the field but have avoided incorporating habitat-specific factors by working with node networks covering a relatively small area, but in this study, we examined the potential to scale up for larger areas and in more complex habitats.

Keywords Calibration, Eastern whip-poor-will, Localization error, Pitch pine, Radio signal strength, Scrub oak, Trilateration

Introduction

In recent decades, documenting animal movements through telemetry has become an increasingly popular method in studying animal ecology. With advancements in remote sensor technology, the accuracy of telemetry data and the scale of its application in research has greatly improved. By minimizing limitations in human labor and bias in field observations, automated telemetry can provide consistent, fine-scale animal locations, as well as other physiological and environmental

*Correspondence:
Marja H. Bakermans
mbakermans@wpi.edu
[1] Department of Biology and Biotechnology, Worcester Polytechnic Institute, Worcester, MA, USA
[2] Massachusetts Division of Fisheries and Wildlife, Westborough, MA, USA
[3] Department of Integrative and Global Studies, Worcester Polytechnic Institute, Worcester, MA, USA

characteristics, such as heart rate and temperature [1–4]. Progressing from their initial use in the 1950s and 1960s, tracking devices have greatly improved in design, such as being more cost-effective, battery-efficient, lightweight, and smaller in size. With this development in technology, previously difficult-to-track animals, both terrestrial and aquatic, have been made possible without impacting the survival of the tagged organism [5, 6]. Current automated tracking systems include the Argos and Motus networks, which utilize GPS and radio signaling, respectively. Depending on the study, tracking tags used in either system can be adjusted in both the device's signal frequency and battery capacity. However, the accuracy of transmitter locations, tracking duration, and geographic scope depends on the study organism, tracking technology employed, and tracking device settings [1].

Both tracking systems allow for detecting long-distance movements of animals, but GPS devices are more accurate and can provide data throughout the year, while Motus-based transmitters are generally smaller in size but signals are only detected in proximity to a Motus receiver (~ 15 km) [6, 7]. Studies that use different kinds of tracking technology are equally valid; however, these systems often fail to accurately capture smaller-scale movements of individuals, like when examining site-level foraging behavior [4]. Studies documenting this type of data previously utilized traditional handheld radio receivers, costing extensive amounts of time and human labor to document locations and location bias associated with human interference from field observations [2, 8]. However, installing multiple automated receivers in a smaller grid, spanning several hundred acres, allows for fine-scale observation of the day-to-day behavior of a target species [9, 10].

In this study, we used the automated radio telemetry system (ARTS) equipment of Cellular Tracking Technologies (CTT). CTT systems function similarly to Motus systems, placing constantly active, solar-powered radio receivers, or "nodes", across a study site to detect tagged animals as they move within the node network. Once deployed, CTT ARTS may provide 'near GPS accuracy' (e.g., ± 30 m) in optimal conditions [11]. Nodes in this system record the radio signal strength (RSS) values of any nearby tags within range and then transmit those data to a nearby central base station for upload to a virtual database. Since RSS values alone provide no information on a tag's location, users must find the rate at which RSS changes depending on the distance of a tag [12–14]. By understanding this relationship, we are able to estimate the distance of a tag from a node based on RSS readings. Following this, we can estimate the position of a tag through trilateration, which uses the approximate distances of a tag retrieved from three or more nodes [13].

Despite similar manufacturing methods for tags and nodes, each device retains a slightly different sensitivity when transmitting or receiving radio signals [15]. Individual nodes in an ARTS may have varying sensitivities to reading radio tag signals. In addition to node deviation, radio signals produced by nodes interact with various complex environmental conditions that affect their propagation. In the case of this study, natural barriers between a node and a tag may disrupt the radio signal between them, generating a margin of error for determining the distance between nodes and tags [6, 12, 13]. Many studies recognize the varying factors that can interfere with ARTS function in an outdoor setting, including radio receiver positioning and setup, temperature, vegetation, and humidity [12, 13, 16–18]. By adjusting for these variables, estimated location accuracy for tags has improved greatly for ARTS research. However, few studies address the issue of telemetry accuracy when dealing with multiple habitat types as opposed to one consistent habitat within a study area.

The goals of this study were to (1) evaluate the relationship of RSS in heterogeneous habitats, (2) estimate locations with trilateration using different models, (3) calculate localization error among models using known locations, (4) visualize the estimated locations, and (5) compare RSS-based locations to GPS data generated from the same individual. More specifically, we evaluated tag and node sensitivity and how heterogeneous habitats influence the accuracy of RSS values when tracking birds with radio telemetry. We studied these questions in a managed scrub oak-pitch pine barren that has four major habitats: treated pitch pine, scrub oak, deciduous hardwood forest, and pitch pine forest [19, 20]. As documented in past studies, signal strength values should decay exponentially as the distance from nodes increases [13, 14]. Overall, we predict that areas with more structurally complex vegetation, such as pitch pine or scrub oak, will hinder signal strength more than more open habitats, like treated pitch pine. Next, we implemented these relationships into a trilateration model with habitat-specific parameters to estimate locations and calculate localization errors with known coordinates. In addition to these tests, we used sample data from an Eastern whip-poor-will (*Antrostomus vociferus*) study to visualize the effects of habitat interference.

Methods

Study location

We conducted this study at the Montague Plains Wildlife Management Area (WMA) in Massachusetts, USA (42.569° N, 72.534° W), a 280-hectare site managed by the Massachusetts Division of Fisheries and Wildlife (MADFW) [21]. As part of their Biodiversity Initiative introduced in 1996, the MADFW utilizes mowing, timber harvesting, and prescribed fire treatments to restore the natural pitch pine-scrub oak community to the site [21]. The area hosts approximately 22 different declining or rare plant and animal species, including the brown thrasher (*Toxostoma rufum*), Eastern whip-poor-will, Eastern towhee (*Pipilo erythrophthalmus*), and prairie warbler (*Setophaga discolor*) [21]. Current habitats of the Montague Plains WMA consist of dense scrub oak stands, pitch pine forests, thinned pitch pine-scrub oak barrens, and mature hardwood forests (Fig. 1) [19, 20]. Pitch pine-scrub oak barrens reflect recent disturbance, featuring an open canopy of primarily pitch pine trees and a basal layer of ankle to waist-high shrubs of oak and birch species [20]. Scrub oak stands consist of overhead thickets of scrub oak and birch species, resulting from a harvested area left untreated for a longer period than a thinned pitch pine region [20]. Pitch pine and hardwood forests indicate untreated regions of Montague Plains WMA, with a relatively open understory and dense canopy [20].

Node network and equipment

For the radio telemetry system, we used Cellular Tracking Technologies (CTT) SensorStation™ (version 2.0), Nodes™ (Version 2.0 with GPS) and PowerTags™ (Generation III PowerTag Digitally Coded Radio Transmitter). The tags weigh about 1.5 g with an estimated battery life of 6 months and transmit a digitally coded UHF radio signal (434 MHz) every 45 s. Nodes were battery and solar powered, allowing for continuous function. We fixed nodes at the top of a 10-foot steel conduit tube (¾ inch) placed 2 feet in the ground. Within the study area, we placed 70 nodes in a grid spaced ~ 200 m apart across approximately 250 hectares (Fig. 2). Nodes transmitted data to the SensorStation every hour, compiling and uploading over the cellular network to an online database.

Tag and node sensitivity and calibration

We measured the radio signal strength of the PowerTags used in the node calibration process. To assess tag sensitivity, we calculated each tag's average RSS and the mean and standard deviation (SD) of the entire dataset. Over a 7-min period using a CTT Locator™ placed 2 m from

Fig. 1 Photos of scrub oak (top left), treated pitch pine (top right), pitch pine (bottom left), and hardwood forest (bottom right) present at Montague Plains WMA (42.569° N, 72.534° W), a managed pine barren. Scrub oak and treated pitch pine photos by Vinh Tran and pitch pine and hardwood forest photos used with permission from Amelia Sadlon

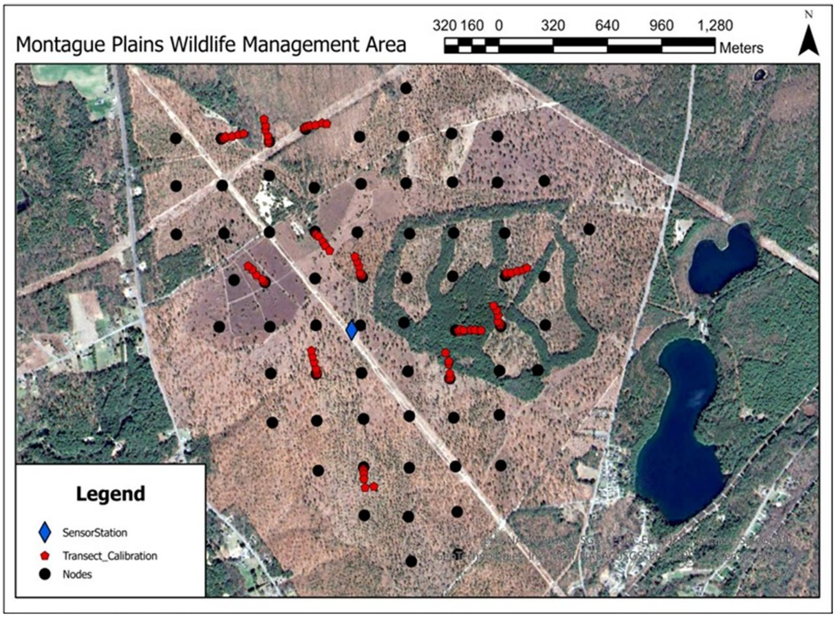

Fig. 2 Map of the study site at Montague Plains WMA, a managed pine barren in western Massachusetts, USA. Equipment at the site includes nodes (black dots), a central data collection station (i.e., SensorStation; blue diamond), and transect points to collect habitat-specific RSS values (red dots)

individual PowerTags, we collected signal measurements [10].

Assessing each node in the network, we recorded radio signal strength using a 2-m tall pole with the PowerTags attached at the top and facing separate directions. We placed the pole 2 m to the north from each node at the site and recorded signals over a 7-min period. Studies that have calibrated ARTS components (e.g., nodes) have used similar or shorter time intervals (e.g., range = 2–8 min); [10, 13, 14, 22]. We calculated node sensitivity by averaging the RSS values of each node and then calculated the mean and standard deviation for the entire dataset. For any tag or node within 1 SD of the mean, we did not adjust RSS readings [14]. For tags or nodes outside of 1 SD, we added a deviation adjustment (difference between values from the individual device and the standard deviation across all nodes) to RSS values from those tags or nodes prior to trilateration [14]. See Bircher et al. on methods of node calibration to account for sensitivity among nodes.

Habitat calibration

To measure habitat-specific RSS in our study site, we established transects from three randomly chosen nodes from each habitat type (Fig. 2). Transects consisted of seven points at distances of 2, 5, 10, 20, 50, 75, and 100 m from the node, with the farthest point being half the distance between nodes, as employed by Paxton et al. We used two 50-m tape measures, a compass bearing to find the correct distances, and a randomly selected cardinal direction for transect point locations. We used the same tag pole for node calibration and collected RSS values over 7-min intervals at each distance from the transect node [13, 14]. We recorded the GPS location of each transect point, placing the handheld GPS (Garmin GPSMAP™ 62sc) at the same location for 7 min to allow for the device accuracy to adjust. We used readings from at least four additional nodes near transect points to increase the number of RSS values across additional distances within the same habitat. The "Generate Near Table" in ArcGIS Pro measured distances between surrounding nodes and transect points. We downloaded data from node memory cards rather than from the SensorStation network, as we found that foliage-dense habitats interfered with uploading complete datasets to the SensorStation.

Negative exponential decay modeling

We described (1) the study system and (2) each habitat type's relationship between RSS and distance using the negative exponential decay function formula:

$$\mathrm{RSS} = a * \exp(-S * \mathrm{distance}) + K$$

where a is the intercept, K is the horizontal asymptote, and S is the decay factor [13]. Of the 12 transects recorded, we randomly selected eight transects (i.e., two for each habitat type) and used their RSS values to generate negative exponential decay functions. We used RSS values from the other four transects to test the estimated location accuracy using these functions (i.e., localization error).

Location estimates and localization error

We modified previously established trilateration techniques to implement our decay functions and generate location estimates [13]. To determine if our calibrations and habitat-specific decay functions increased trilateration accuracy, we created several different localization models using these adjustments. We developed three localization models: one using a single negative exponential decay function without considering habitat interference (null model), one with only the node calibration adjustments (node model), and another using negative exponential decay functions of each habitat (habitat model). Using the habitat model as an example, it includes the decay function parameters for each habitat, switching between each function depending on a node's location. Furthermore, for each model, we generated location estimates using RSS-based filters, selecting for RSS readings stronger than a specific signal strength [13]. One filter does not restrict any RSS values (− 110 dB), one filter limits values by the K value of the null function (− 102 dB), and one filter restricted by the highest K value of all decay functions (− 95 dB). Applying these restrictions examined whether models would reflect improved accuracy without substantial data loss by selecting for stronger signal readings [13]. To ensure that we used all available data, we collected RSS values from both the SensorStation and memory cards from each node.

To compare trilateration models, we calculated and compared localization error, the distance in meters between the coordinates of the known location and the estimated location. We used transect points not included in generating the negative exponential decay functions to estimate these localization errors.

Statistical analyses

Negative exponential decay modeling—We used a nonlinear regression analysis to test for differences in negative exponential decay models between the null model and habitat model (nls() function) [23] using all RSS readings from the habitat calibration. First, we fit a model that constrains the parameters (a, S, and K) to be the same regardless of the group (i.e., null model). Next, we fit another model that estimates separate parameters by group (i.e., habitat model) and then compared models with an F-test [23]. If statistically significant, we ran post-hoc tests on each parameter by habitat with function pairComp() using the Holm method to adjust p-values for multiple comparisons (package aomisc) [24].

Localization error—We generated descriptive statistics to examine the mean localization error by RSS filters, models, and the number of nodes used to estimate locations. We used two-way ANCOVA to test for differences in localization error by RSS filter (i.e., − 95, − 102, and − 110 dBs) and model (e.g., null, node, habitat) while controlling for the number of nodes used to estimate the location. The data adhered to assumptions of normality and homogeneity of variances, requiring no transformations. If the ANCOVA was statistically significant, we ran post-hoc tests to determine which groups differed with function emmeans() using the Holm method to adjust p-values for multiple comparisons (package emmeans) [25].

All statistical analyses were performed in R (ver. 4.2.1; [26]). Data and R code from this study are available in the Zenodo repository [27].

Sample application

We used 2022 data from a male whip-poor-will fitted with a CTT PowerTag to visually compare different RSS filters and models with the same dataset. Because we do not have a dataset of directly observed sightings for this individual, this visualization is to reflect any data loss, patterns, or changes in location estimates observed rather than to further test filter and model accuracy. To simplify the visualization, we only included RSS data from one individual taken from June 5th to June 11th, representing part of the prime breeding period for this species [28]. Using the post-hoc ANCOVA results, we used ArcGIS Pro to map whip-poor-will locations for models that significantly differed along with the simplest model (e.g., fewest adjustments) with significant differences.

In a pilot study examining breeding home ranges of whip-poor-wills, we placed a GPS data logger (PinPoint 10, 1.2 g, Lotek Wireless) on this same individual male, collecting GPS-derived locations from 25 May to 29 June 2020. We mapped these locations in Google Earth Pro to visualize habitat types used by this whip-poor-will and as a comparison to locations generated through this study, given that this male demonstrated site fidelity (i.e., the same banding location) across at least five breeding seasons [29, 30].

Results

Tag and node sensitivity and calibration

We originally used four tags in the field for node calibration; however, one tag malfunctioned during data collection and was not retained in this study. The three remaining tags had an average RSS of − 47.45 dB (3.74 SD). Mean RSS for individual tags (i.e., − 46.57, − 47.85, and − 47.93 dBs) fell within 1 SD and, thus, did not require additional calibration.

We measured 70 nodes in the 2022 field season across Montague Plains WMA, with an average RSS of −45.8 dB (SD ± 4.3 dB) and recorded 15 nodes outside of 1 SD (Fig. 3).

Habitat calibration and negative exponential decay models

Of the nodes deployed at Montague Plains WMA, we randomly selected 12 nodes for habitat transects, with eight used in calibration and four used in testing the estimated locations. We plotted 275 averaged RSS values (total 5505 readings) from eight transects among habitats, which produced a null exponential decay model of −53.99*exp(−0.0122 *distance) −101.82 (Table 1, Fig. 4). For the models of each habitat type, pitch pine resulted in −60.12*exp(−0.0126 *distance) − 103.98, hardwood forest was −53.78*exp(−0.0079*distance) − 107.91, treated pitch pine −49.14*exp(−0.0198*distance) − 95.29, and scrub oak −58.61*exp(−0.0110*distance) − 105.08 (Table 1, Fig. 5).

The parameters of the habitat-specific models differed from the null model ($F_{9,263} = 6.76$, $p < 0.001$). Post-hoc analyzes that account for multiple comparisons revealed that the hardwood habitat decay factor (S) differed from pitch pine ($t = -3.5$, $p = 0.003$; Appendix 1) and a marginal difference between scrub oak and pitch pine ($t = -2.56$, $p = 0.052$). The horizontal asymptote (K) for pitch pine differed from all other habitat types (hardwood: $t = -4.77$, $p < 0.001$; scrub oak: $t = -5.69$, $p < 0.001$; treated pitch pine: $t = -4.40$, $p < 0.001$). Lastly, there was a significant difference in intercept between treated pitch pine and pitch pine ($t = -2.79$, $p = 0.032$) and a marginal difference between scrub oak and pitch pine ($t = -2.45$, $p = 0.069$).

Table 1 Parameters from negative exponential decay modeling

Habitat	Parameter	Coefficient	SE
All habitats	*a*	53.99	1.42
	S	0.0122	0.0009
	K	− 101.82	0.82
Pitch pine	*a*	60.12	2.60
	S	0.0126	0.0019
	K	− 103.98	1.68
Hardwood	*a*	53.78	0.32
	S	0.0079	0.0014
	K	− 107.91	2.73
Treated pitch pine	*a*	49.14	3.10
	S	0.0198	0.0035
	K	− 95.29	0.99
Scrub oak	*a*	58.61	2.06
	S	0.0110	0.0010
	K	− 105.08	0.01

Beta estimates and standard errors (SE) for the parameters a (intercept), S (decay factor), and K (horizontal asymptote) in negative exponential decay modeling. The null model combined data from all habitats, and the habitat model estimated parameters by habitat type. Data were used to understand the relationship between receiver signal strength (RSS) and distance of a radio tag from a node and were collected in a managed pine barren in western Massachusetts (USA) in summer 2022

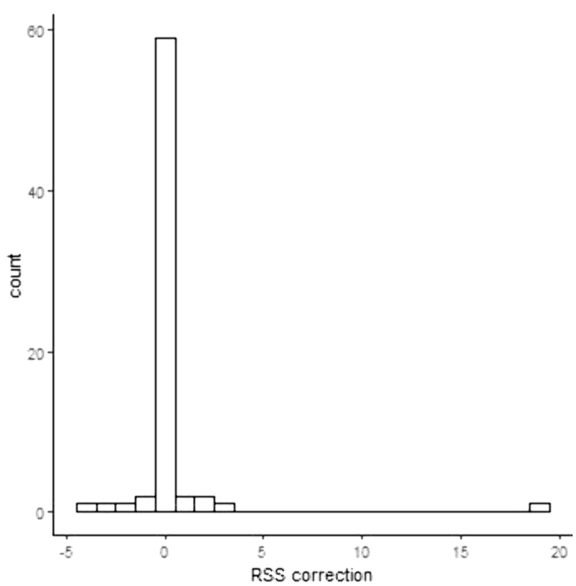

Fig. 3 Histogram of radio signal strength (RSS, dB) corrections for 70 nodes at a pine barren in western Massachusetts (USA). Any node in the zero bin was within 1 SD of the mean RSS readings and did not require a correction

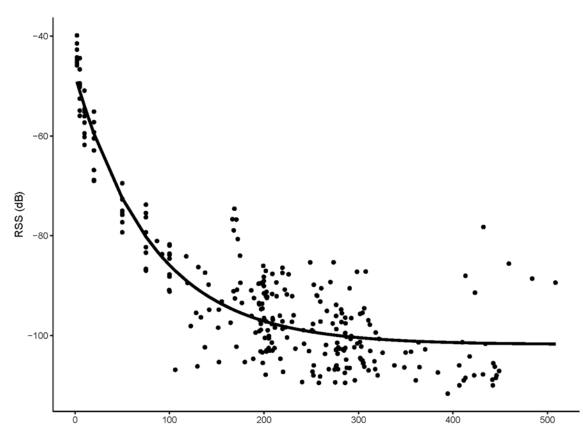

Fig. 4 A negative exponential decay model was generated from transect calibration points, with all habitat types combined (i.e., null model). Transects ran in a random cardinal direction from two randomly chosen nodes per habitat type at distances of 2, 5, 10, 20, 50, 75, and 100 m from the node. Receiver signal strength (RSS) and distance of a radio tag from a node were collected in a managed pine barren in western Massachusetts (USA) in summer 2022

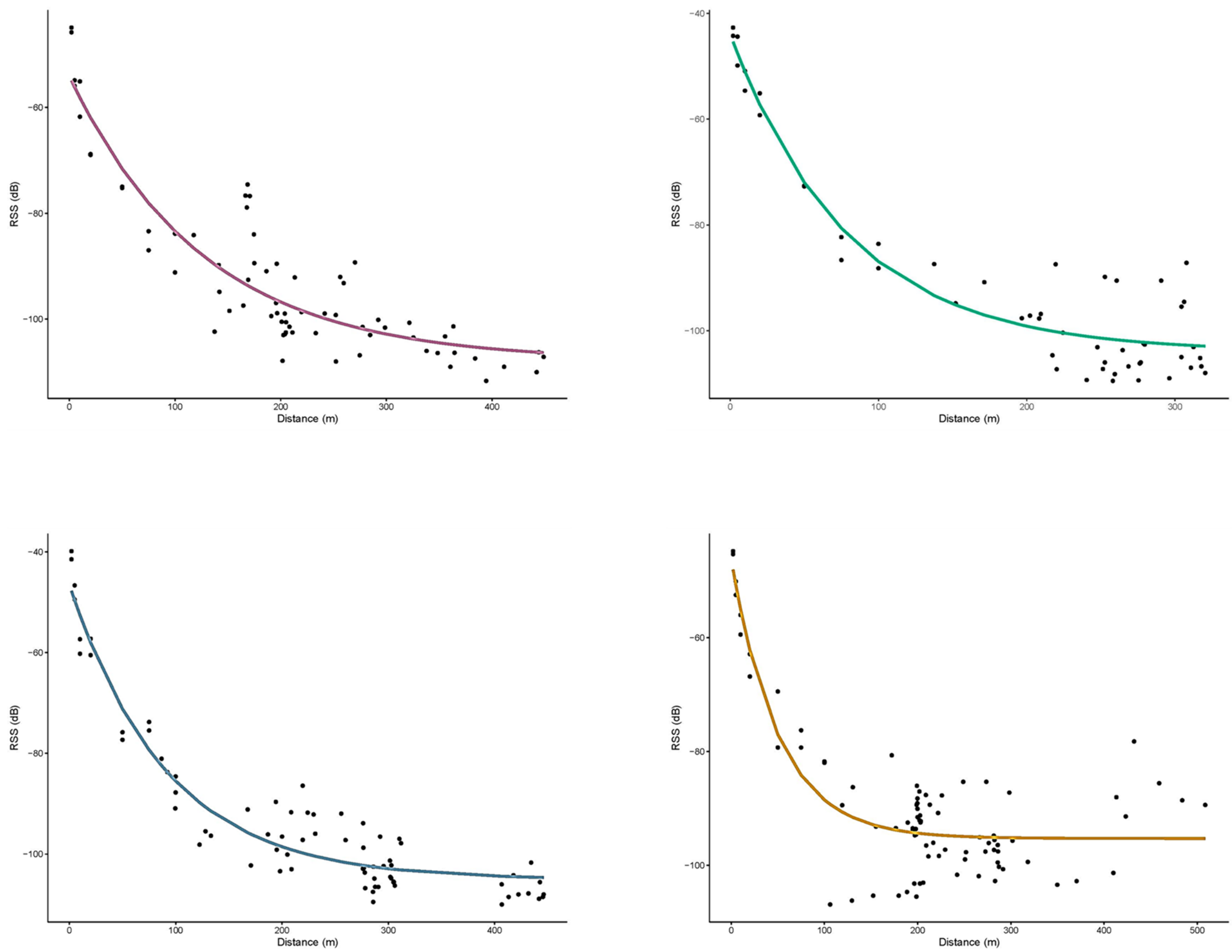

Fig. 5 Negative exponential decay models for each habitat type, including hardwood forest (upper left), pitch pine (upper right), scrub oak (bottom left), and treated pitch pine (bottom right). Receiver signal strength (RSS) and distance of a radio tag from a node were collected in a managed pine barren in western Massachusetts (USA) in summer 2022

Table 2 Descriptive statistics of localization error

RSS filter	Habitat model	Node model	Null model
−95 dB	46.1 (7.6 SE, $n=8$)	46.3 (7.1 SE, $n=8$)	49.5 (6.6 SE, $n=8$)
−102 dB	59.7 (8.2 SE, $n=20$)	77.7 (10.0 SE, $n=23$)	75.9 (10.0 SE, $n=23$)
−110 dB	65.3 (9.8 SE, $n=22$)	79.0 (10.5 SE, $n=23$)	77.3 (10.6 SE, $n=23$)

Descriptive statistics (mean, SE, and sample size) of the localization error (difference in meters between true and estimated locations) by RSS filter and model. Data were collected in a managed pine barren in western Massachusetts (USA) in summer 2022

Location estimates and localization error

Using four transects to test localization error, the mean distance was the smallest for the −95 dB RSS filter and habitat model combination (46.1 m+−7.6 SE) and greatest for the −110 dB RSS filter and node model combination (79 m+/−10.5 SE; Table 2). However, the strictest RSS filter (i.e., −95 dB RSS filter) resulted in a 75% loss of data, with a 100% loss within the closed canopy locations (i.e., hardwood and pitch pine forests). For the −102 dB RSS filter, we lost 25% of the data, but the estimated measures of error were lower than the no filter (i.e., −110 dB) results. The greater the number of nodes used in the analyses, the smaller the localization error, with the largest decrease in localization error occurring between 3 and 5 nodes (Fig. 6). We excluded any location estimates containing only < 3 nodes ($n=16$) from analyses.

Two-way ANCOVA analyses revealed a statistically significant difference in localization error by model ($F_{2,148}=6.2$, $p=0.003$) and filter ($F_{2,148}=12.8$, $p<0.001$), while their interaction is not significant ($F_{4,148}=0.6$, $p=0.677$). When applying the −102 dB RSS filter, the habitat model differs from both node ($p_{adj}=0.025$) and null ($p_{adj}=0.046$) models (Fig. 7). There is marginal significance between habitat and node ($p_{adj}=0.055$) and

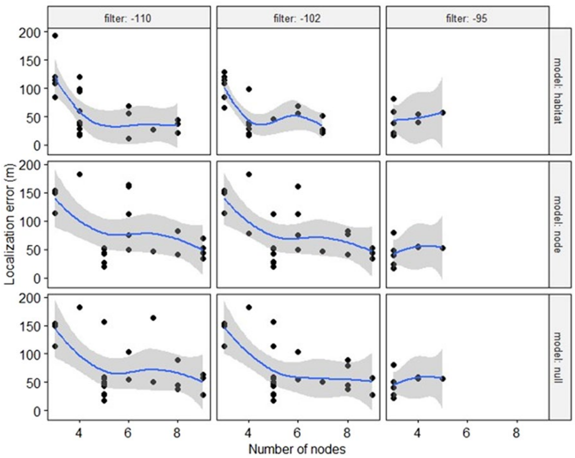

Fig. 6 Localization error (the distance in meters between the coordinates of the known location and the estimated location) in relation to the number of nodes, RSS filter, and model used to generate the locations of known test points. Data were collected from 70 nodes placed in a grid (~200 m apart) in a managed pine barren in western Massachusetts (USA) in summer 2022

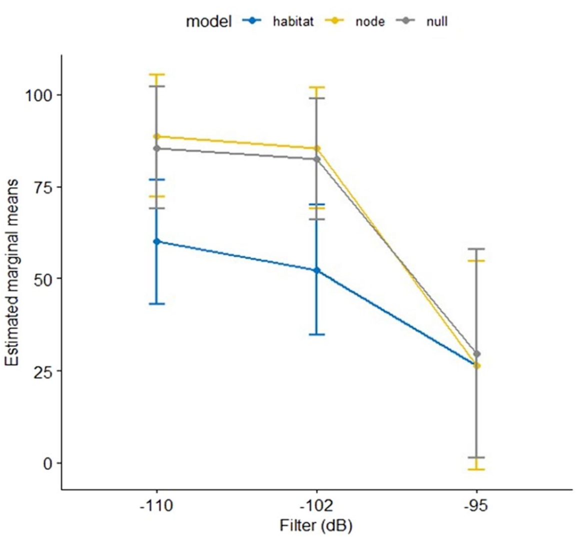

Fig. 7 Estimated marginal means of the localization error in relation to RSS filters and models. Estimated marginal means represent the average of the localization error for each level of predictor variable (filter and model) and are used to assess the simple main effects of model and filter at different levels

null ($p_{adj}=0.069$) models with the −110 dB filter (Fig. 7). None of the models differed with the −95 dB filter (all $p_{adj}=1.000$; Fig. 7). Post-hoc comparisons also revealed that the localization error for the node model at −95 dB significantly differs from the errors with the −102 dB ($p_{adj}=0.001$) and −110 dB filters ($p_{adj}<0.001$, Fig. 7). Likewise, the localization error of the null model with the −95 dB filter is significantly different than errors at the −102 dB ($p_{adj}=0.004$) and −110 dB filters ($p_{adj}=0.003$, Fig. 7). Localization error for the habitat model did not statistically differ among the filters (all $p_{adj}>0.129$).

Sample application

Over a one-week period between 5 June 2022 and 11 June 2022, we were able to estimate 6355 locations of a male whip-poor-will using the least restrictive filter and model (i.e., −110 dB filter and null model). We mapped the results of four models (−110 dB null, −110 dB habitat, −102 habitat, and −95 dB null; Fig. 8) based on the results of the post-hoc ANCOVA tests. Maps of locations indicated 73% data loss when comparing the least restrictive RSS filter (i.e., −110 dB) to the most restrictive RSS filter (i.e., −95 dB). When comparing maps created with null models while adjusting for habitat, we see that the habitat models retained locations in the vegetation-dense habitats with both the −102 and −110 dB RSS filters. Clustering of locations is apparent in areas of pitch pine and treated pitch pine that coincides with locations documented for the same individual in a prior breeding season with GPS technology (Fig. 9).

Discussion

This study addresses a need for additional analyses of big data and bio-logging collection systems in the field under differing conditions [1, 4, 31]. Our results demonstrate that the relationship between a radio transmitter's detected signal strength and distance to a receiver can differ by habitat type. As expected, habitats with dense vegetation interfere with radio signals, causing the signal strength to weaken more rapidly over distance, with pitch pine forests demonstrating the greatest interference. Knowing that habitat type can impact a radio transmitter's detected RSS value, it is important to account for different habitats to increase accuracy when estimating transmitter location.

Our reported values of localization error are within the ranges of those reported for studies with similar (~200 m) spacing among nodes [13, 22]. However, Paxton et al. [13] investigated further reducing localization errors by reducing node spacing and creating simulated grids with 100, 175, and 250-m spacings. Their study found that the closest spacing (100 m) led to the greatest significant decrease in localization error. Tilson [10] and Wallace et al. [32] also document this effect using grids with node spacing of approximately 25 m and 10–74 m apart, respectively. Though these studies greatly reduced their localization errors, with Tilson [10] reporting 13.2 m and Wallace et al. [32] reporting 7 m, it is important to note their study sites were much smaller, covering

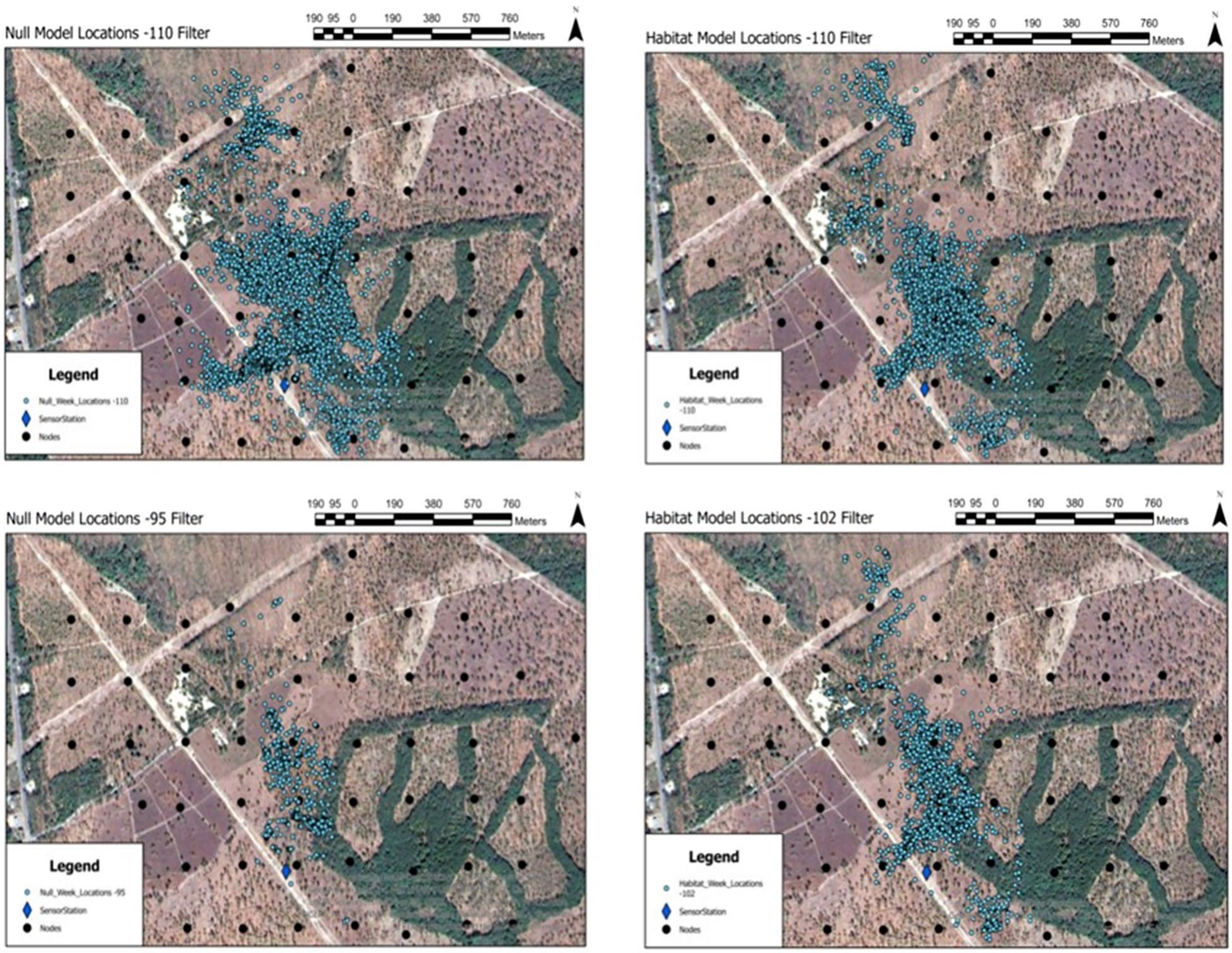

Fig. 8 Trilateration estimates of a male eastern whip-poor-will over a 7-day period (5–11 June 2022) at a managed pine barren in western Massachusetts (USA). Maps include point locations generated using − 110 dB RSS filter and null model (top left, $n=6355$ points), − 110 dB RSS filter and habitat model (top right, $n=4139$), − 95 dB RSS filter and null model (bottom left, $n=1742$ points), and − 102 dB RSS filter and habitat model (bottom right, $n=3245$ points)

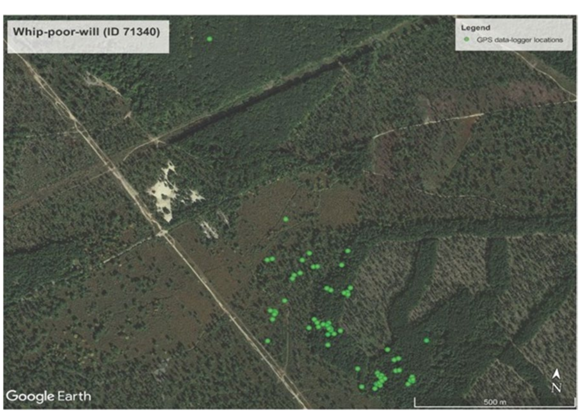

Fig. 9 GPS data logger-derived locations ($n=70$) from the same individual (BirdID = 71340) from 25 May to 29 June 2020, as displayed in Google Earth Pro

approximately 2.0 and 0.4 hectares, respectively. As with most animal tracking equipment, the tracking grid used in our study has limitations. While reducing node spacing can reduce location error, this approach would be costly and time-consuming when covering a large area like our study site. Additionally, most animal movements outside of the established array of nodes go undetected, and locations estimates may be unreliable [22]. Also, our study was conducted at a single site, resulting in no replication at the site level.

When estimating locations, we found that across all models, a range of three to five nodes used for trilateration provided the greatest improvement in accuracy, with a slight decrease in error as more nodes were added. Tilson [10] documented a continued decrease in error as the number of nodes increased (up to 16) in their study. Furthermore, when comparing the localization error of our different models (i.e., node, habitat, and null) using known locations, the habitat model provided the best combination of improved accuracy while minimizing data loss. In addition, the node model failed to improve localization accuracy compared to the null model. Thus, we do not see a need for node calibration moving forward with research on whip-poor-wills in this study area, and it may not be necessary for other studies.

Studies have documented artificial patterns when comparing estimated locations to known (or test) locations. Mostly, studies noted that estimated locations were pulled to the center of the node network [13, 22, 33]. Bil et al. [9] found that estimated locations were cluttered at equal distances between nodes when implementing a habitat-specific calibration curve. In our study, we noticed that points occasionally formed an empty circular pattern around nodes, suggesting that some points close to nodes could not be mapped correctly despite efforts to adjust and calibrate RSS readings. This pattern was most pronounced in our vegetation-dense pitch pine habitat. Similar to our study, Paxton et al. [13] found that RSS-based filters can minimize these artificial patterns.

However, implementing RSS filters that are too strict without accounting for habitat-specific decay will likely bias estimated locations. RSS filters that have been used in studies included −88 dB [9], −90 dB [10], −95 dB [13], and −100 dB [22]. The most stringent RSS filter used in our study (−95 dB) provided significantly less localization error in all models but greatly reduced the number of estimated locations. In fact, all locations in the hardwood forests and pitch pine forests were lost when employing the −95 dB filter. Thus, using our most restrictive filter and not considering habitat would bias the interpretation of a species' habitat use or selection because location estimates may be lost in areas where radio transmission is degraded. Alternatively, applying a filter slightly above the K values of our most dense habitat types provided an effective decrease in localization error with minimal data loss. Furthermore, at our study site, highly accurate GPS locations clearly illustrate that whip-poor-wills utilize multiple habitat types, including pitch pine, indicating that trilateration calculations of this species should account for habitat type. For other studies focused on species that utilize multiple habitat types, we suggest accounting for this source of error while also applying limited RSS filtering when estimating locations using radio telemetry. Working in uniform or open habitats, like grasslands, may not require habitat calibration measures as applied in our study.

It is clearly established that field-based ARTS have various sources of interference besides those related to habitat type [8, 12, 34]. Therefore, consideration of each factor depends on the study subject and location, the time and resources available for calibration, and the level of precision desired. For instance, our study, like Tilson [10], did not consider the elevation change of an animal or of a node since the study site is nearly uniform in elevation. For studies at a site with extensive topographic variation, the elevation change across the site may impact a telemetry system's signal transmission and reception [8, 22, 34]. Though it has been highlighted that many sources of location error are involved in using ARTS, these systems are highly versatile to the desired needs of research projects. Depending on the level of precision desired, the quantity, spacing, and elevation of nodes and the tag size and signal transmission rate can be modified to cater to research objective needs [13, 22, 33, 34].

Conclusion

Implementing an ARTS has greatly expanded the research opportunities on animals, particularly for those that are small and difficult-to-study species, like Eastern whip-poor-will [28]. Radio telemetry technology has been used to study whip-poor-will to better understand home range size, habitat use, and territorial movements [35–40], but an automated approach that can collect data at any time of the day or night should provide a better understanding of their movement patterns and ecology. The next steps for this project on Eastern whip-poor-will breeding ecology include using calibration measures to estimate the locations of birds on the breeding grounds, generating home ranges, and examining habitat use and movements in relation to habitat management (e.g., prescribed burns and mechanical treatments). Although, the setup and calibration of such networks are time-consuming and strenuous, especially if habitats are difficult to traverse. When calibrating the system, several sources of error may add additional challenges, such as malfunctioning tags, nodes, or memory cards (e.g., corrupt files), and these limitations were present in our study. Despite these obstacles, accounting for calibration in varying habitats should improve the capability and information provided by automated radio telemetry systems in future studies.

Appendix

Pairwise comparisons of parameters from negative exponential decay models by habitat. Parameters include intercept (a), decay factor (S), and horizontal asymptote (K). Habitat groups are indicated by the numbers in the table and include hardwoods (1), treated pitch pine (2), scrub oak (3), and pitch pine (4). We ran post-hoc tests on each parameter by habitat with function pairComp() using the Holm method to adjust p-values for multiple comparisons (package aomisc; Onofri 2020). Pairs that are significantly different are indicated with bold font.

Parameter and Pair	Estimate	SE	*t* value	Pr(>|*t*|)
a1-a2	−6.338	3.938	−1.610	0.430
a1-a3	−4.836	3.841	−1.259	0.624
a1-a4	−4.638	4.066	−1.141	0.324
a2-a3	−1.503	3.709	−0.405	0.685
a2-a4	**−10.977**	**3.941**	**−2.785**	**0.032**
a3-a4	−9.474	3.845	−2.464	0.069
S1-S2	−0.005	0.002	−2.124	0.135
S1-S3	−0.003	0.002	−1.808	0.164
S1-S4	**−0.012**	**0.003**	**−3.510**	**0.002**
S2-S3	−0.002	0.002	−0.713	0.476
S2-S4	−0.007	0.004	−1.923	0.164
S3-S4	−0.009	0.003	−2.559	0.052
K1-K2	−3.923	3.032	−1.294	0.587
K1-K3	−2.827	2.873	−0.984	0.650
K1-K4	**−12.617**	**2.645**	**−4.769**	**<0.000**
K2-K3	−1.069	2.270	−0.483	0.650
K2-K4	**−8.694**	**1.975**	**−5.694**	**<0.000**
K3-K4	**−9.790**	**1.719**	**−5.694**	**<0.000**

Acknowledgements
We are extremely grateful to numerous volunteers and students for their assistance with fieldwork and lab meeting discussions. In particular, we would like to thank Joshua Driscoll, Natalie Kay, Amelia Sadlon, and Zoë Swartley. We thank Luke DeGroote for providing advice and code. We thank the journal reviewers for their thoughtful feedback and efforts toward improving our manuscript.

Author contributions
VTT—project conception, design, and management; data curation, collection, and analysis; manuscript writing—original draft, review, and editing; visualization. ACV—funding; project conception and design; data collection; manuscript writing—review and editing. MHB—funding; project conception, design, and management; data collection and analysis; manuscript writing—original draft, review, and editing; visualization.

Funding
This work was funded by the Massachusetts Division of Fisheries and Wildlife, Massachusetts Department of Transportation Linking Landscapes for Massachusetts Wildlife Program, Wildlife and Sport Fish Restoration Program administered by the United States Fish and Wildlife Service, and with support from the Biology and Biotechnology Department at WPI.

Availability of data and materials
The datasets generated and/or analyzed during the current study are available in the Zenodo repository: https://doi.org/10.5281/zenodo.10965575.

Declarations

Ethics approval and consent to participate
All fieldwork involving animals was approved by the Institutional Animal Care and Use Committee of Worcester Polytechnic Institute (protocol no. 20-119) and was conducted under a US Geological Survey Bird Banding Laboratory banding permit issued to A. Vitz (no. 21963-S).

Consent for publication
Authors (VTT, ACV, MHB) consent to the publication of this manuscript.

Competing interests
No, I declare that the authors have no competing interests as defined by BMC, or other interests that might be perceived to influence the results and/or discussion reported in this paper.

Received: 21 January 2024 Accepted: 23 April 2024
Published online: 03 May 2024

References

1. Trappes R. How tracking technology is transforming animal ecology: epistemic values, interdisciplinarity, and technology-driven scientific change. Synthese. 2023;201(4):128. https://doi.org/10.1007/s11229-023-04122-5.
2. Katzner TE, Arlettaz R. Evaluating contributions of recent tracking-based animal movement ecology to conservation management. Front Ecol Evol. 2020;7:519. https://doi.org/10.3389/fevo.2019.00519.
3. Whitford M, Klimley AP. An overview of behavioral, physiological, and environmental sensors used in animal biotelemetry and biologging studies. Anim Biotelemetry. 2019;7(1):1–24. https://doi.org/10.1186/s40317-019-0189-z.
4. Cagnacci F, Boitani L, Powell RA, Boyce MS. Animal ecology meets GPS-based radiotelemetry: a perfect storm of opportunities and challenges. Philos Trans Royal Soc B: Biol Sci. 2010;365(1550):2157–62. https://doi.org/10.1098/rstb.2010.0107.
5. Cooke SJ, Midwood JD, Thiem JD, Klimley P, Lucas MC, Thorstad EB, Eiler J, Holbrook C, Ebner BC. Tracking animals in freshwater with electronic tags: past, present and future. Anim Biotelemetry. 2013;1:1–9. https://doi.org/10.1186/2050-3385-1-5.
6. Taylor PD, Crewe TL, Mackenzie SA, Lepage D, Aubry Y, Crysler Z, Finney G, Francis CM, Guglielmo CG, Hamilton DJ, Holberton RL. The motus wildlife tracking system: A collaborative research network to enhance the understanding of wildlife movement. Avian Conservation and Ecology. 2017. https://doi.org/10.5751/ACE-00953-120108.
7. Douglas DC, Weinzierl R, Davidson SC, Kays R, Wikelski M, Bohrer G. Moderating Argos location errors in animal tracking data. Methods Ecol Evol. 2012;3(6):999–1007. https://doi.org/10.1111/j.2041-210X.2012.00245.x.
8. Lenske AK, Nocera JJ. Field test of an automated radio-telemetry system: tracking local space use of aerial. J Field Ornithol. 2018;89(2):173–87.
9. Bil W, Asso AA, Van Eekelen P, Both C, Ouwehand J. Living on the forest edge: flexible habitat use in sedentary Pied Flycatchers *Ficedula hypoleuca* during the non-breeding season. Ardea. 2023;111(1):371–96. https://doi.org/10.5253/arde.2022.a38.
10. Tilson D. Emerging technology for the study of one of North America's most elusive birds, the black rail (*Laterallus jamaicensis*). [dissertation]. Athens, Georgia (USA): University of Georgia; 2022.
11. Cellular Tracking Technology. CTT Node User Guide. 2023. https://cellular-tracking-technologies.github.io/ctt_documentation/CTT-Node-User-Guide.pdf. Accessed 12 Dec 2023.
12. Luomala J, Hakala I. Analysis and evaluation of adaptive RSSI-based ranging in outdoor wireless sensor networks. Ad Hoc Netw. 2019;87:100–12. https://doi.org/10.1016/j.adhoc.2018.10.004.
13. Paxton KL, Baker KM, Crytser ZB, Guinto RMP, Brinck KW, Rogers HS, et al. Optimizing trilateration estimates for tracking fine-scale movement of wildlife using automated radio telemetry networks. Ecol Evol. 2022;12(2):e8561. https://doi.org/10.1002/ece3.8561.
14. Bircher N, Van Oers K, Hinde CA, Naguib M. Extraterritorial forays by great tits are associated with dawn song in unexpected ways. Behav Ecol. 2020;31(4):873–83. https://doi.org/10.1093/beheco/araa040.
15. Triguero-Ocaña R, Vicente J, Acevedo P. Performance of proximity loggers under controlled field conditions: an assessment from a wildlife ecological and epidemiological perspective. Animal Biotelemetry. 2019. https://doi.org/10.1186/s40317-019-0186-2.
16. Luomala J, Hakala I. Effects of temperature and humidity on radio signal strength in outdoor wireless sensor networks. In Federated Conference on Computer Science and Information Systems (FedCSIS) 2015 Sep 13 (pp. 1247–1255). IEEE.

17. Ward MP, Sperry JH, Weatherhead PJ. Evaluation of automated radio telemetry for quantifying movements and home ranges of snakes. J Herpetol. 2013;47(2):337–45. https://doi.org/10.1670/12-018.
18. Heim KC, Ardren WR, Castro-Santos T. Using recovered radio transmitters to estimate positioning error and a generalized Monte Carlo simulation to incorporate error into animal telemetry analysis. Anim Biotelemetry. 2023;11(1):26. https://doi.org/10.1186/s40317-023-00337-y.
19. Akresh ME, King DI. Eastern whip-poor-will breeding ecology in relation to habitat management in a pitch pine-scrub oak barren. Wildl Soc Bull. 2016;40(1):97–105. https://doi.org/10.1002/wsb.621.
20. Motzkin G. The vegetation of Montague Plains Wildlife Management Area, 1993–2016: Changes over 23 years and responses to management. Massachusetts Division of Fisheries and Wildlife. 2016. https://harvardforest1.fas.harvard.edu/publications/pdfs/Motzkin_Montague_2016.pdf. Accessed 15 Feb 2023.
21. Simmons T, Hawthorne B. Montague Plains Wildlife Management Area: Montague, Massachusetts. Massachusetts Division of Fisheries and Wildlife. 2014 Jan. https://www.mass.gov/doc/montague-plain-wma-site-plan/download. Accessed 15 Feb 2023.
22. Russell E. Habitat associations and fine-scale movements of the Red-Spotted Toad (*Anaxyrus punctatus*) in Kansas and the efficacy of remote telemetry for monitoring small-scale movements [thesis]. Hays, Kansas (USA): Fort Hays State University; 2023. https://doi.org/10.58809/TGSN5167
23. R Core Team. A language and environment for statistical computing. In: The R Project for Statistical Computing. 2022. https://www.R-project.org/.
24. Ritz C, Streibig JC, editors. Nonlinear regression with R. New York: Springer, New York; 2008.
25. Onofri A. The broken bridge between biologists and statisticians: a blog and R package. https://github.com/OnofriAndreaPG/aomisc. 2020. Accessed 21 Sep 2022.
26. Lenth R. Estimated Marginal Means, aka Least-Squares Means. In: Package emmeans. 2023. https://cran.r-project.org/web/packages/emmeans/emmeans.pdf Accessed 4 Dec 2023.
27. Tran VT, Vitz AC, Bakermans MH. Dataset for evaluating habitat-specific interference in automated radio telemetry systems: implications for animal movement studies. 2024. Zenodo. https://doi.org/10.5281/zenodo.10965575.
28. Cink CL, Pyle P, Patten MA. Eastern Whip-poor-will (Antrostomus vociferus). In: Rodewald PG, editor. Birds of the World. Cornell Lab of Ornithology; 2020. https://doi.org/10.2173/bow.whip-p1.01
29. Bakermans MH, Driscoll JM, Vitz AC. Habitat selection and site fidelity on winter home ranges of Eastern Whip-poor-wills (*Antrostomus vociferus*). Avian Conserv Ecol. 2022;17(2):17. https://doi.org/10.5751/ACE-02237-170217.
30. Bakermans MH, Vitz AC. Hot stops: timing, pathways, and habitat selection of migrating eastern whip-poor-wills. J Avian Biol. 2023. https://doi.org/10.1111/jav.03142.
31. Whitehouse K, Karlof C. Culler D A practical evaluation of radio signal strength for ranging-based localization. ACM SIGMOBILE Mobile Comput Commun Rev. 2007;11(1):41–52. https://doi.org/10.1145/1234822.1234829.
32. Wallace G, Elden M, Boucher R, Phelps S. An automated radiotelemetry system (ARTS) for monitoring small mammals. Methods Ecol Evol. 2022;13(5):976–86. https://doi.org/10.1111/2041-210X.13794.
33. Baldan D, van Loon EE. Songbird parents coordinate offspring provisioning at fine spatio-temporal scales. J Anim Ecol. 2022;91(6):1316–26. https://doi.org/10.1111/1365-2656.13702.
34. Rutz C, Morrissey MB, Burns ZT, Burt J, Otis B, St Clair JJH, et al. Calibrating animal-borne proximity loggers. Methods Ecol Evol. 2015;6(6):656–67. https://doi.org/10.1111/2041-210X.12370.
35. Stewart S. Temporal space use dynamics and full breeding cycle survival rates of Eastern whip-poor-wills in Illinois [dissertation]. Urbana, Illinois (USA): University of Illinois Urbana-Champaign; 2023. https://hdl.handle.net/2142/120236
36. Spiller KJ, King DI, Bolsinger J. Foraging and roosting habitat of Eastern Whip-poor-wills in the northeastern United States. J Field Ornithol. 2022. https://doi.org/10.5751/JFO-00057-930106.
37. Souza-Cole I. Understanding the diel activity patterns and determinants of abundance of the Eastern whip-poor-will. [dissertation]. Urbana, Illinois (USA): University of Illinois Urbana-Champaign; 2021. http://hdl.handle.net/2142/112998
38. Grahame ERM, Martin KD, Gow EA, Norris DR. Diurnal and nocturnal habitat preference of eastern whip-poor-wills (Antrostomus vociferous) in the northern portion of their breeding range. Avian Conserv Ecol. 2021;16(2):14. https://doi.org/10.5751/ACE-01929-160214.
39. Hunt PD. Extra-territorial movements by Eastern whip-poor-wills. North Am Bird Bander. 2016;41(3):97–102.
40. Wilson MD, Watts BD, Paxton BJ. An investigation of Whip-poor-will activity, habitat use, and home range using radio telemetry within a managed landscape. CBTR-02–11. Center for Conservation Biology Technical Report Series. College of William and Mary, Williamsburg, VA. 50 pp. 2022. https://scholarworks.wm.edu/cgi/viewcontent.cgi?article=1424&context=ccb_reports. Accessed 15 Nov 2023.

Publisher's Note